Spike sorting based on automatic template reconstruction with a partial solution to the overlapping problem

Pu-Ming Zhang [a,b,1], Jin-Yong Wu [a], Yi Zhou [b], Pei-Ji Liang [b], Jing-Qi Yuan [a,c,*]

[a] *Department of Automation, Shanghai Jiao Tong University, Shanghai 200030, China*
[b] *Department of Biomedical Engineering, Shanghai Jiao Tong University, Shanghai 200030, China*
[c] *State Key Laboratory of Bioreactor Engineering/ECUST, Shanghai 200237, China*

Abstract

A new method for spike sorting is proposed which partly solves the overlapping problem. Principal component analysis and subtractive clustering techniques are used to estimate the number of neurons contributing to multi-unit recording. Spike templates (i.e. waveforms) are reconstructed according to the clustering results. A template-matching procedure is then performed. Firstly all temporally displaced templates are compared with the spike event to find the best-fitting template that yields the minimum residue variance. If the residue passes the χ^2-test, the matching procedure stops and the spike event is classified as the best-fitting template. Otherwise the spike event may be an overlapping waveform. The procedure is then repeated with all possible combinations of two templates, three templates, etc. Once one combination is found, which yields the minimum residue variance among the combinations of the same number of component templates and makes the residue pass the χ^2-test, the matching procedure stops. It is unnecessary to check the remaining combinations of more templates. Consequently, the computational effort is reduced and the over-fitting problem can be partly avoided. A simulated spike train was used to assess the performance of the proposed method, which was also applied to a real recording of chicken retina ganglion cells.
© 2003 Elsevier B.V. All rights reserved.

Keywords: Spike sorting; Template-matching; χ^2-Test; Overlapping; Principal component analysis; Subtractive clustering

1. Introduction

Multi-unit extracellular recordings contain spike streams of several neurons adjacent to the electrodes. Spikes from different neurons may overlap temporally and produce distorted waveforms, and noise inevitably distorts spike waveforms. Therefore, it is necessary to decipher the multi-unit recordings to find out the number of neurons contributing to each electrode recording, as well as the characteristic waveforms (templates) and the spike temporal sequence of each neuron.

The spike sorting problem has received intense attention and a large number of techniques have been developed. However, many methods have concentrated on the detection and

classification of the spikes by assuming that the templates were known a priori (Salganicoff et al., 1988; Sarna et al., 1988; Zouridakis and Tam, 1997; Lewicki, 1998; Letelier and Weber, 2000), while only a few methods have dealt with templates creation. Atiya (1992) used the Isodata clustering algorithm to estimate the typical spike shapes, and then compared all possible combinations of the templates to find the combination with the highest likelihood. This procedure, however, has the drawback of being computationally expensive, particularly when the number of overlapping is high. In addition, the over-fitting problem is unavoidable. Lewicki (1994) applied Bayesian probability theory to define a probabilistic model of the waveform and to quantify the probability of both the form and the number of spike shapes. This method was also used to deduce an efficient algorithm for the decomposition of arbitrarily complex overlapping sequences, and it was more computationally efficient than that of Atiya (1992). Zouridakis and Tam (2000) proposed a procedure based on fuzzy *K*-means clustering algorithms to identify the exact number of neurons contributing to a

* Corresponding author. Tel.: +86-21-62932031;
fax: +86-21-62932145.
E-mail addresses: pmzhang@sjtu.edu.cn (P.-M. Zhang),
jqyuan@sjtu.edu.cn (J.-Q. Yuan).
[1] Tel.: +86-21-64070495; fax: +86-21-64070495.

multi-unit recording and to create reliable spike templates. Pouzat et al. (2002) developed a procedure for the classification and validation of extracellular data based on a probabilistic model of data generation. An empirical characterization of the recording noise was used to optimize the clustering of recorded events into putative neurons, and also to assess the quality of each cluster. However, their spike classification method was the same as that of Atiya (1992).

Here we present a new spike-sorting approach based on automatic template reconstruction with a partial solution to the overlapping problem. Firstly, principal component analysis (PCA) and subtractive clustering techniques are used to estimate the number of neurons contributing to the multi-unit recording. The spike templates are reconstructed according to the clustering results. The template-matching procedure is then performed on the records together with the χ^2-test to sort spikes. Every template with possible temporal displacement is compared with the spike event to find the best-fitting template. If the residue passes the χ^2-test, the matching procedure for this spike event stops and the spike event is classified as the best-fitting template. Otherwise, the spike event may be an overlapping waveform. The procedure is then repeated with all possible combinations of two, three, or more templates to decompose the overlapping waveform. Once a combination is found to be the best-fitting one among the combinations of the same number of templates and it makes the residue pass the χ^2-test, the matching procedure stops and the overlapping waveform is classified as this combination. It is unnecessary to check the remaining combinations of more templates. As a result, the computational effort is reduced. The proposed approach was tested with both simulated data and a segment of real data to assess its performance.

2. Methods

2.1. Data collection

2.1.1. Real data

The experiments were carried out on the isolated, newly hatched (about 2–4 days) chicken retinas with multi-electrode array (MEA, Multi Channel System MCS GmbH, Germany) (Chen et al., 2003). The retinal segments were attached with the ganglion cell side to the surface of the multi-electrode array. Multi-unit photoresponses were recorded from all 60 electrodes simultaneously, which were amplified with a 60-channel amplifier (single-ended amplifiers, bandwidth 10 Hz–3.4 kHz, amplification 1200). The recording was digitized with a commercial multiplexed data acquisition system (MCRack) and stored in a Pentium-based computer. MCRack sampled the incoming data at a rate of 20 kHz, and stored the data for offline analysis.

Here the recordings from single electrodes are analyzed. Some general assumptions in our method are as given further.
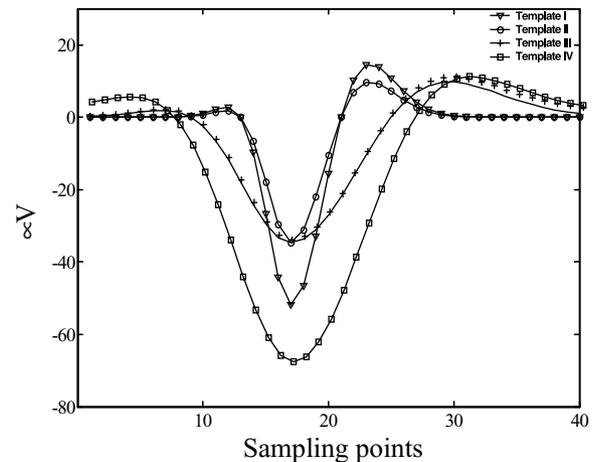

Fig. 1. Standard templates stimulating the spikes of four retinal ganglion cells.

(1) The spike waveforms generated by a neuron are time-invariant. Since the isolated retinal segments were attached to the surface of multi-electrode array and the experiment lasted only for 3–4 min, only little changes in the spike waveforms were observed.
(2) The noise follows Gaussian distribution (Atiya, 1992; Lewicki, 1994).
(3) The spike events and the noise are statistically independent (Pouzat et al., 2002).
(4) The single spikes add linearly to produce overlapping waveforms.

2.1.2. Simulated data

The simulated signal has some advantages over the real signal for evaluating the performance of the algorithm, because it provides known solutions under different conditions, such as real templates, firing time and so on.

The simulated spike train was designed by using four spike templates and background noise. The spike train lasted for 1 s (20,000 sampling points when the sampling frequency is 20 kHz). The spike templates are shown in Fig. 1, which simulate the spikes of four retinal ganglion cells. Thirty-five instances of each template were randomly added to the background noise. For each template, the inter-spike interval of each instance followed an exponential distribution (the temporal sequence of each template is a Poisson train).

The background noise was taken from a segment of a real recording. After the spike events were extracted from the recording of a selected electrode, the noise traces were concatenated and regarded as the background noise (Fig. 2A).

The simulated spike train shown in Fig. 2B simulated four neurons firing independently. There were 14 overlapping waveforms, among which 12 waveforms were the overlapping of two templates and 2 waveforms were the overlapping of three templates (as shown in Table 1).
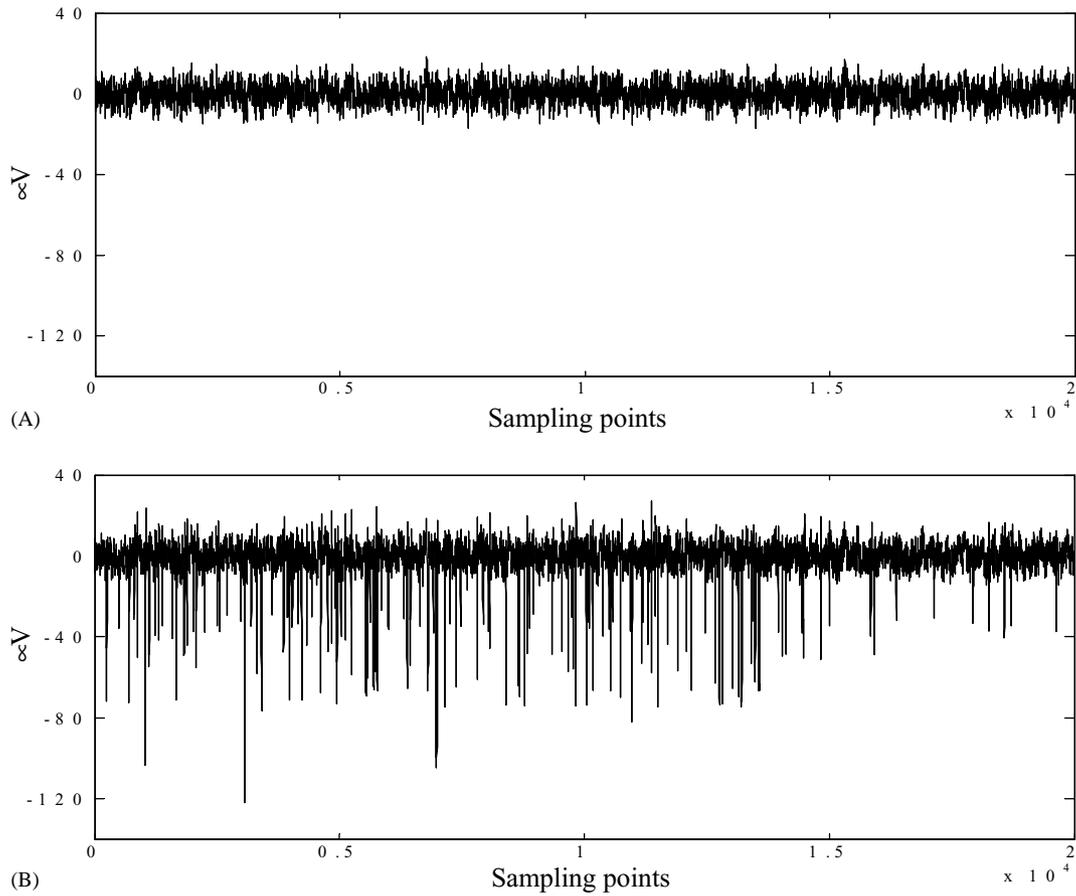
Fig. 2. Simulated spike train. Thirty-five instances of each template were randomly added to the background noise, and the temporal sequence of each template was a Poisson train. (A) Background noise. (B) The simulated spike train.

2.2. Spike template reconstruction

2.2.1. Spike events detection and features extraction

Extracellular recordings of retinal ganglion cells spikes are usually characterized by initial sharp negative troughs, so in this study, when a negative peak exceeds a preset threshold, a fixed length of waveform (40 sampling points, 16 points before and 23 points after the peak) is extracted from the recording. Such waveform is defined as a spike event y_i, $y_i \in R^{1 \times 40}$. All detected spike events produce a data set Y, $Y \in R^{n \times 40}$, where n is the number of spike events.

Principal component analysis (PCA) is used to extract features from the data set Y.

$$Y = SL^{\mathrm{T}} = \sum_{i=1}^{n} s_i l_i^{\mathrm{T}} \tag{1}$$

Table 1
Sorting results of the simulated spike train

Component templates of spike events	Number of spike events	Our method		Atiya's method	
		Number of wrongly classified spike event	Wrongly classified as template	Number of wrongly classified spike event	Wrongly classified as template
I	28	0		1	I, II[a]
II	27	1	I	1	I
III	27	0		1	II, III[a]
IV	28	0		0	
I, II	4	1	II, III	1	II, III
I, III	2	0		0	
I, IV	1	0		0	
II, III	1	0		0	
II, IV	1	1	I, IV	1	I, IV
III, IV	3	0		1	II, III, IV[a]
II, III, IV	2	0		0	

[a] These three spike events were over-fitted by Atiya's method.

where L is the principal component loadings matrix and S the principal component scores matrix. In this study, the scores of the first two principal components serve as the features for spike events classification.

2.2.2. Spike events classification and templates reconstruction

The scatter plot of the scores of the first two principal components is analyzed by the subtractive clustering method (Chiu and Cheng, 1994) to reveal the classification of spike events. There are n data points in the scatter plot, which refer to n spike events. Those data points are defined as z_i $(i = 1, \ldots, n)$.

In the subtractive clustering method, rough estimates of the local population densities are used to determine cluster centers in a serial fashion. The density $D_1(z_i)$ at data point z_i $(i = 1, \ldots, n)$ is

$$D_1(z_i) = \sum_{j=1}^{n} \exp\left\{-\frac{||z_i - z_j||^2}{(\gamma_a/2)^2}\right\} \tag{2}$$

where γ_a is a resolution parameter specified by the user. The data point with the highest local density is considered to be the first cluster center. Let z_1^* denote the first cluster center and let $D_1(z_1^*)$ denote the density at z_1^*. In the next step, z_1^* is removed and the density at z_i is updated by discounting the contribution of z_1^* as follows:

$$D_2(z_i) = D_1(z_i) - D_1(z_1^*)\exp\left\{-\frac{||z_i - z_1^*||^2}{(\gamma_b/2)^2}\right\} \tag{3}$$

where γ_b is another resolution parameter specified by the user. The value of γ_b is chosen to be larger than that of γ_a to avoid the cluster centers to be too close to one another. At this step, the second cluster center z_2^* is found, whose density is the maximum among all $D_2(z_i)$. Let $D_2(z_2^*)$ denote the density at z_2^*. The density for finding the $(j + 1)$th $(j = 2, 3, \ldots)$ cluster center is defined as

$$D_{j+1}(z_i) = D_j(z_i) - D_j(z_j^*)\exp\left\{-\frac{||z_i - z_j^*||^2}{(\gamma_b/2)^2}\right\} \tag{4}$$

This process is repeated until the density of the remaining points is smaller than a predetermined threshold (Chiu and Cheng, 1994).

The number of clusters, defined as M, reflects the number of neurons contributing to the recording. Here a circle with radius r_k is used to describe the cluster whose center is z_k^*. The radius r_k is defined by the user. The template of each neuron is then reconstructed as the average waveform of the spike events belonging to each cluster. Since the aim at this stage is to reconstruct templates, in order to guarantee the accuracy of the templates, the value of r_k should be chosen appropriately. It should be small enough to ensure that each cluster is separated from the others without overlapping. However, it cannot be too small. Otherwise the noise cannot be restrained by the averaging method, or the

reconstructed templates become some special spike events. The appropriate value of r_k can be deduced from the scatter plot by the user.

2.3. Template-matching with a partial solution to overlapping problem

After the template of each neuron has been reconstructed, the template-matching procedure is then employed to identify spikes in the recording and reveal the spike temporal sequence of each neuron.

2.3.1. χ^2-Test for template-matching

The noise in extracellular recordings is approximated as Gaussian noise with a variance of σ^2 and a mean of zero. σ^2 can be estimated from idle (non-spiking) periods of the recording (Atiya, 1992).

The spike event is generated by a template or templates combination, so that after the template or templates combination is subtracted from the spike event, the residue contains only noise. Since it is a segment of the Gaussian noise, the unbiased estimation of its variance v^2 must be the same as σ^2. If we define W as the length of the residue, the ratio of $(W - 1)v^2$ to σ^2 is a random variable which follows the χ^2 distribution with $(W - 1)$ degree of freedom, i.e.,

$$\frac{(W-1)v^2}{\sigma^2} \sim \chi^2(W-1) \tag{5}$$

The hypothesis-testing problem is defined as follows:

$$H_0 : v^2 = \sigma^2 \quad \text{against} \quad H_1 : v^2 \neq \sigma^2$$

The test statistic θ is chosen as follows:

$$\theta = \frac{(W-1)v^2}{\sigma^2} \tag{6}$$

Given the significance level α of rejection of H_0, H_0 is accepted if and only if

$$\chi^2_{1-\alpha/2}(W-1) < \theta < \chi^2_{\alpha/2}(W-1) \tag{7}$$

For example, if $\alpha = 0.2$, $W = 80$, then $\chi^2_{1-\alpha/2}(W-1) = 64.1564$, $\chi^2_{\alpha/2}(W-1) = 96.4872$. If the value of θ is within the range $(64.1564, 96.4872)$, H_0 is accepted, which means the residue passes the χ^2-test. Therefore, the spike event is classified as the template or templates combination.

2.3.2. Template-matching procedure

The template-matching procedure is to search for the template or templates combination that satisfies the conditions as given further.

(1) The number of templates matched to each spike event is the minimum. This is to avoid possible over-fitting.
(2) Among the templates (or templates combinations that have the same number of component templates), the matched template (or templates combination) yields the minimum residue variance.

(3) After the matched template (or templates combination) is subtracted from the spike event, the residue passes the χ^2-test.

Because of noise, the peak of each spike event may not be the real peak of the template. In particular, overlapping can distort or even obliterate the spike waveform of each component neuron. Therefore, the template must be shifted in a much wider window around the spike event peak to find its real position. Here the window width is set as 80 sampling points (36 points before and 43 points after the peak of the spike event), i.e., $W = 80$.

The matching procedure begins from single-template-matching. If a template with proper temporal displacement can fit the spike event better than other single templates with any displacement (i.e., compared with other single templates with any displacement, this template with proper temporal displacement yields the minimum residue variance), and the residue passes the χ^2-test, then the matching procedure for this spike event stops. As a result, the spike event is classified as this best-fitting template, and the firing time is defined by the temporal displacement.

Otherwise, the spike event may be an overlapping waveform. Firstly all possible combinations of every two templates are checked. If a pair templates combination with proper temporal displacement yields better-fitting than other pair templates combinations with any displacement (i.e., compared with other pair templates combinations with any displacement, this pair templates combination with proper temporal displacement yields the minimum residue variance), and the residue passes the χ^2-test, the matching procedure for this spike event stops. As a result, the spike event is classified as this best-fitting pair templates combination, and the firing time of each template is defined by its temporal displacement.

If the residue cannot pass the χ^2-test, the procedure is repeated with all possible combinations of every three templates, four templates, etc. Once a combination of templates satisfying the above three conditions is found, the matching procedure stops. It is unnecessary to check the remaining combinations of more templates. As a result, the computational effort is reduced.

If all tests fail, which means no template or templates combination can satisfy all of the three conditions, the event is classified as the template or templates combination that yields the minimum residue variance among all possible combinations.

3. Results

The proposed procedure was firstly applied to simulated data, and then to real data recorded from the chicken retina. All of the data were analyzed offline using a personal computer (Celeron 1.7 GHz, 256 MB RAM) using MATLAB 6.1. All the routines are available upon request.
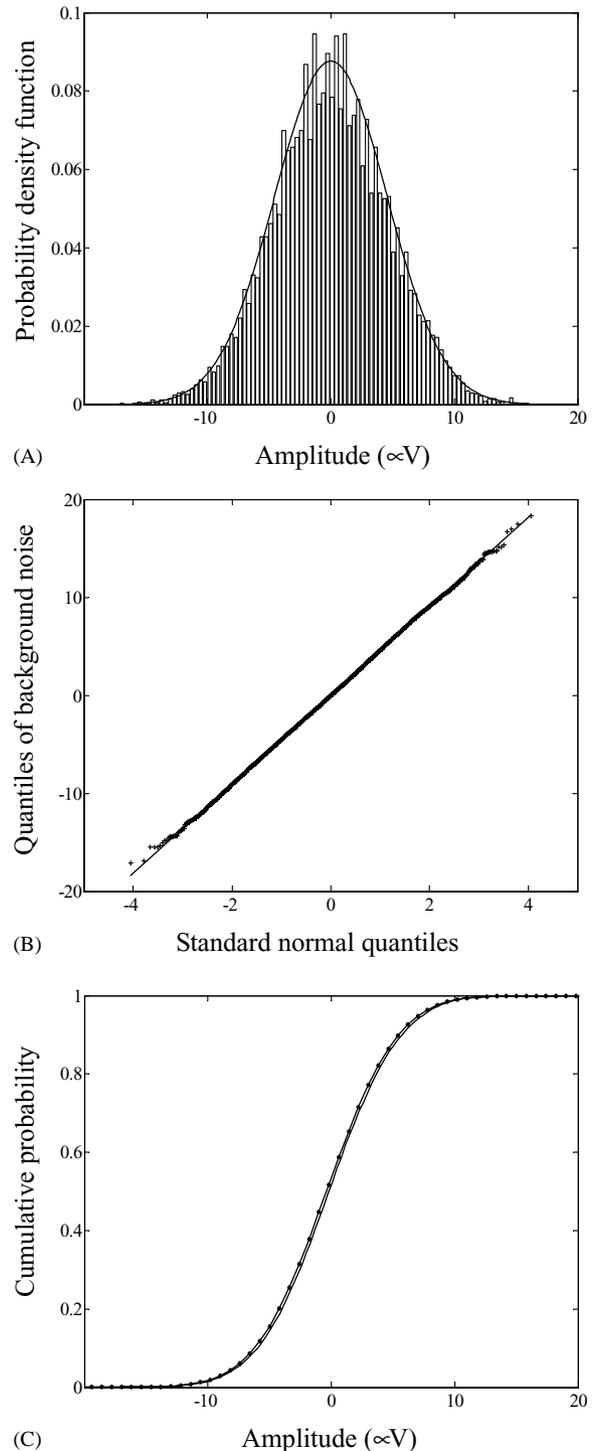

Fig. 3. (A) The background noise amplitude histogram. The histogram is the probability density estimated from the noise, and the curve is the expected Gaussian probability density. (B) The quantile–quantile plot of the quantiles of background noise versus the quantiles of a standard normal distribution. (C) The cumulative probability distribution obtained from the noise is shown by solid curve, and the expected Gaussian distribution is shown by dotted curve. The three figures show that the noise followed Gaussian distribution with a mean of 0.0017 and an S.D. of 4.5532.

3.1. Application to simulated data

3.1.1. Statistical properties of noise

The amplitude histogram of the background noise is shown in Fig. 3A. The quantile–quantile plot of the quantiles of the noise versus the quantiles of a standard normal distribution is shown in Fig. 3B. The cumulative probability distribution of the noise is shown in Fig. 3C. These figures show that the noise followed Gaussian distribution with a mean of 0.0017 and a standard deviation (S.D.) of 4.5532.

3.1.2. Spike sorting results

In the simulated signal, there were 142 peaks detected by setting the threshold of the peak value as $-25.0\,\mu\text{V}$. The threshold value was proper, so no inserted spike was missed and no spurious spike event was detected. Since the noise and overlapping distort the waveforms, a spike event may have more than one detected peak. As a result, there were 124 spike events, which produced the spike events data set $Y \in R^{124 \times 40}$.

The data set Y was processed by PCA. Scores of the first two principal components were then analyzed by the sub-tractive clustering method. The clustering result is shown in Fig. 4A. Four clusters were identified, which means the number of neurons contributing to the spike train was four. Consequently, the template of each neuron was reconstructed as shown in Fig. 4B. Fig. 4C shows a spike event corresponding to the point Pa in Fig. 4A. It was distorted little by the noise, so its corresponding point Pa is in the central area of the corresponding cluster. Those unclassified points in Fig. 4A were bias, which might be noise, overlapping waveforms, or badly distorted spikes. For example, the point Pb in Fig. 4A was such an unclassified point, whose corresponding spike event was an overlapping waveform as shown in Fig. 4D.

The proposed template-matching procedure was carried out step by step. While proceeding the χ^2-test, the significance level α was set as 0.20. The sorting results are shown in Table 1. Among the 124 spike events, 121 spike events were correctly classified and the other three were wrongly classified. One spike event generated by template II was wrongly classified as template I, one spike event generated by templates I and II was wrongly classified as templates II and III, one spike event generated by templates II and IV was wrongly classified as templates I and IV. Although the
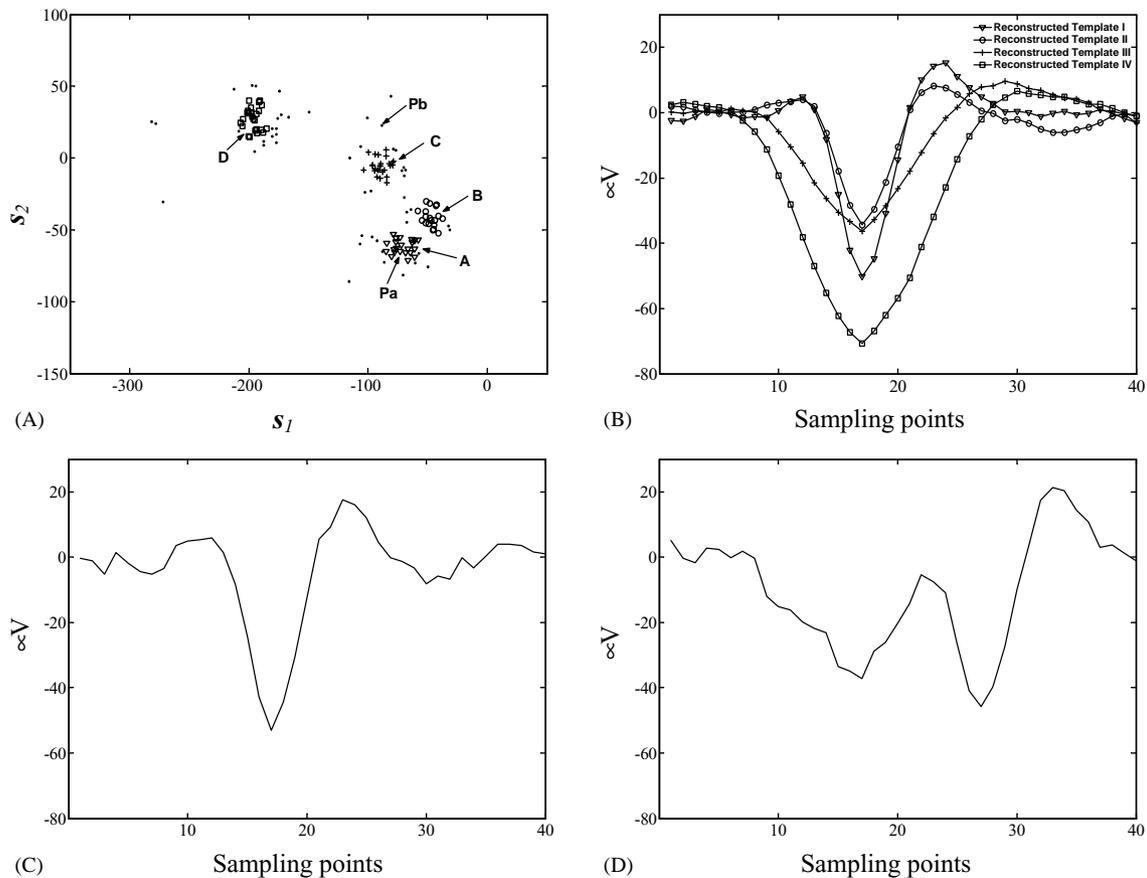

Fig. 4. Templates reconstruction. (A) Scatter plot of scores s_1 and s_2 of the first two principal components. These principal components accounted for 87.6% of the data variation. After being analyzed by subtractive clustering method ($\gamma_a = 0.2$, $\gamma_b = 0.25$, the radius of each cluster was 15), four clusters were identified, i.e. (A–D). (B) Reconstructed templates. Reconstructed template I was the average waveform of the spike events belonging to cluster A, reconstructed template II–IV belonging to cluster (B–D), respectively. (C) The spike event corresponding to the point Pa in (A). It was generated by the standard template I and was distorted little by noise, so the corresponding point was in the cluster's central area. (D) The spike event corresponding to the point Pb in (A). It was an overlapping waveform, so the corresponding point was a bias point.
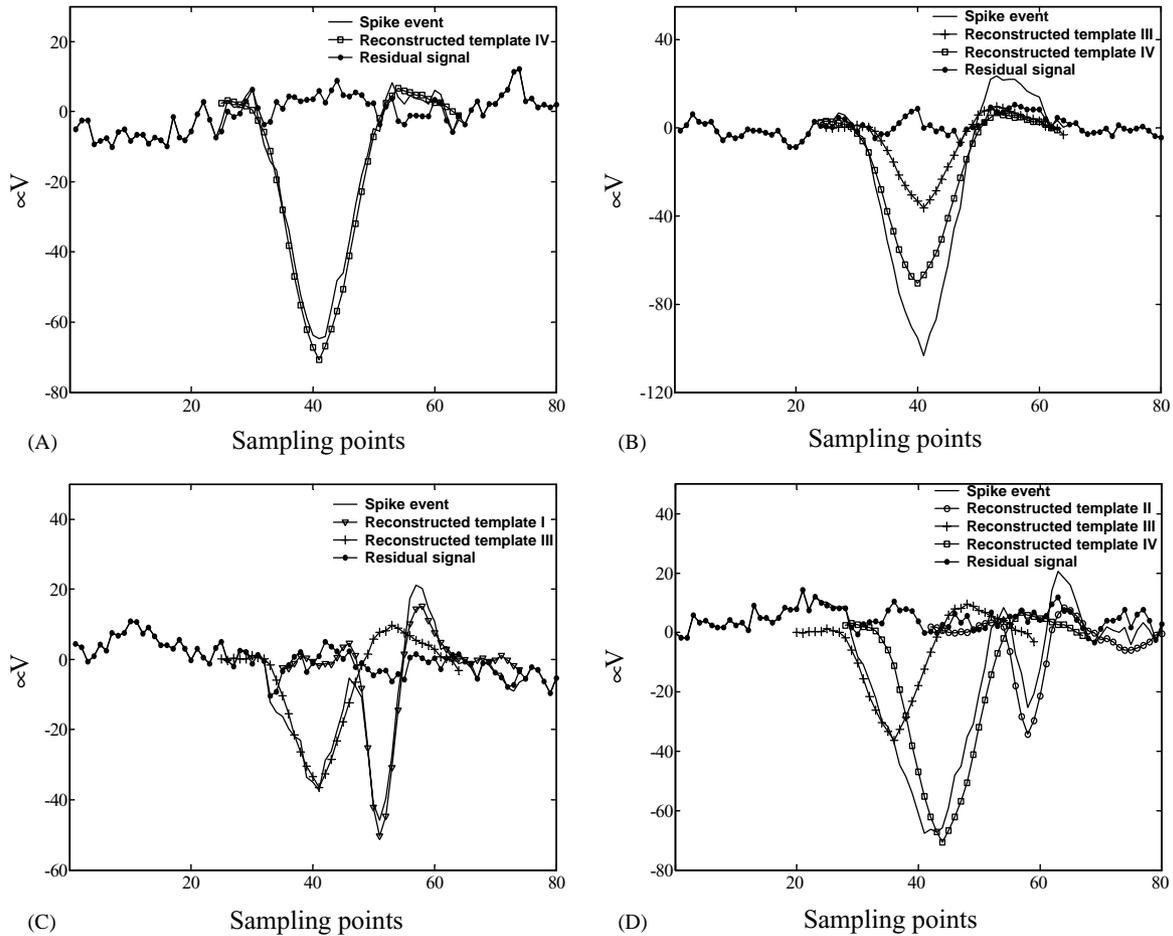
Fig. 5. Examples of spike sorting results. (A) This spike event was classified as reconstructed template IV. The value of θ was 95.5189, which was within the range (64.1564, 96.4872), so the residue passed the χ^2-test and this event was well classified. (B) This spike event was classified as the combination of reconstructed templates III and IV. The value of θ was 71.0063, which was within the range (64.1564, 96.4872), so the residue passed the χ^2-test and this event was well classified. (C) This spike event was classified as the combination of reconstructed templates I and III. The value of θ was 76.0636, which was within the range (64.1564, 96.4872), so the residue passed the χ^2-test and this event was well classified. (D) This spike event was classified as the combination of reconstructed templates II–IV. The value of θ was 46.8078, which was out of the range (64.1564, 96.4872), so the residue did not pass the χ^2-test. Finally this event was forced to be classified as the three templates combination that yielded the minimum variance of the residue. By comparing it with the original true template sequences, we know this sorting result was correct.

sorting results were not perfect, the accuracy of 121/124 was still acceptable. Four examples are shown in Fig. 5. After subtracting all of the classified templates from the simulated signal, the residue shown in Fig. 6 followed the Gaussian distribution with a mean of 0.1927 and an S.D. of 4.5852. It was a little different from the background noise, because three spike events were classified wrongly and those reconstructed templates were still distorted to some extent by the noise.

As comparison, Atiya's method (1992) was also employed and the results are shown in Table 1. Among the 124 spike events, six spike events were wrongly classified, three of which were wrongly classified the same as in our method, and three were over-fitted. One example of the over-fitting is shown in Fig. 7. This spike event was generated by template III. Our proposed method classified it well as shown in Fig. 7A, while Atiya's method classified it as the combination of templates II and III as shown

in Fig. 7B. The method proposed in this paper therefore seems to be more efficient to overcome the over-fitting problem.

To evaluate the spike sorting results, the degree of misalignment of correctly matched reconstructed-templates is defined as follows:

$$\Delta = \frac{\sum_{i=1}^{M} \sum_{j=1}^{m_i} |t_{i,j} - \hat{t}_{i,j}|}{\sum_{i=1}^{M} m_i} \tag{8}$$

where $\hat{t}_{i,j}$ is the peak time of the ith reconstructed-template at the jth correctly matched time; $t_{i,j}$ is the true peak time of the corresponding ith template at the jth time; m_i is the number of the correctly matched instances of the ith reconstructed-template. In the results of our method, 28 spike events generated by template I were correctly classified, six overlapping waveforms generated by template I and another template were correctly decomposed. As
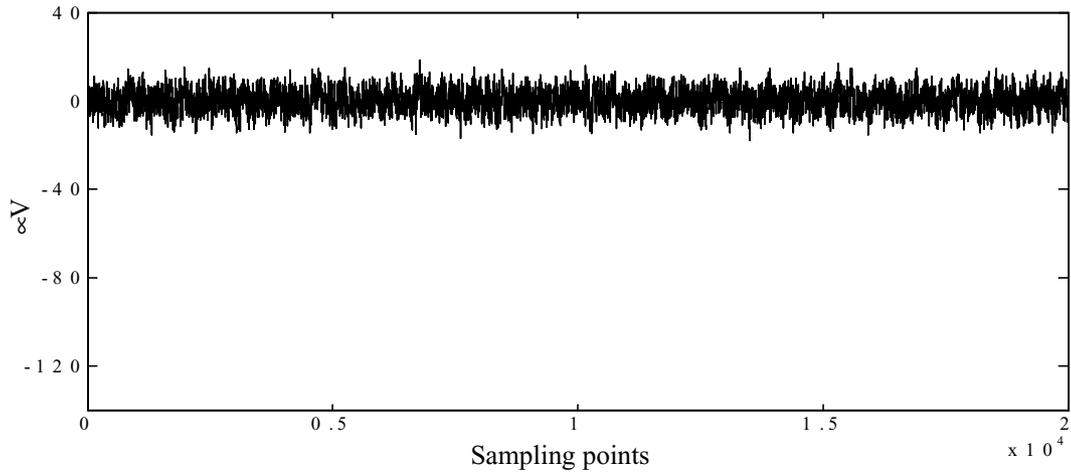
Fig. 6. Residue of the simulated signal after all of the classified templates being subtracted.

Table 2
Performance comparison

	Our method	Atiya's method
Δ	33/137	39/137
Computation efforts (s)	232.7	3391.9

a result, m_1 was 34. In the same way, m_2 was 33, m_3 was 35 and m_s was 35. In the results of Atiya's method, one spike event generated by template I was classified as the combination of templates I and II. Although it was an over-fitting, we still regarded this template I as one correctly matched template I. Together with 27 correctly classified spike events which were generated by template I and six correctly decomposed overlapping waveforms which were generated by template I and another template, m_1 was 34. In the same way, m_2 was 33, m_3 was 35 and m_4 was 35.

Table 2 reveals that Atiya's method is time consuming and the misalignment is more serious than that of our method.

3.2. Application to real data

Here the proposed procedure was applied to real data recorded from an isolated, newly hatched chicken's retina in darkness (no light stimulus). The recording of one selected electrode is shown in Fig. 8. The sampling frequency was 20 kHz and this segment of recording lasted for 10 s. The noise was estimated from the idle periods of the recording, which followed the Gaussian distribution with a mean of 0.0977 and an S.D. of 5.9197.

There were 147 spike events detected by setting the threshold of the peak-to-peak value as 20 μV. The scatter plot of the scores of the first two principal components as well as the clustering result are shown in Fig. 9A. Two clusters were identified, which means that there were two ganglion cells contributing to the recording. Their spike waveforms (templates) were reconstructed as shown in Fig. 9B.

Then the template-matching procedure proceeded step by step. As a result, there were 67 spike events classified as
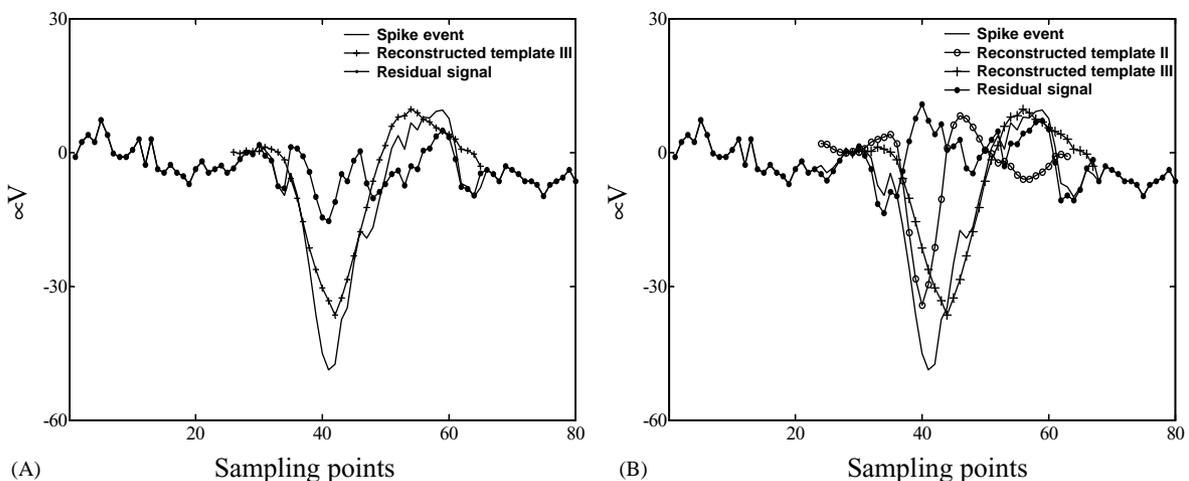

Fig. 7. (A) The spike event was well classified by the proposed method. (B) The spike event was over-fitted by Atiya's method.
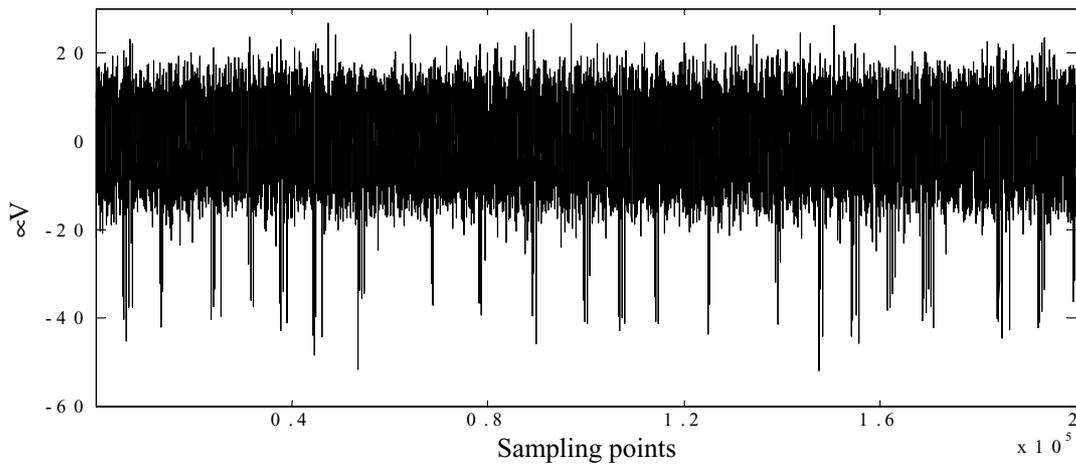
Fig. 8. Responses of the chicken retinal ganglion cells recorded from one electrode in darkness. The sampling frequency was 20 kHz. The segment of recording lasted for 10 s. After all of the possible spike events were subtracted from the recording, the noise trace was obtained by connecting the idle periods of the recording. The noise followed the Gaussian distribution with a mean of 0.0977 and an S.D. of 5.9197.

template I, 53 spike events as template II, and 27 spike events were overlapping waveforms. Two examples are shown in Fig. 10. After subtracting all of the classified templates from the recording, we got the residue. The residue followed the Gaussian distribution with a mean of 0.0836 and an S.D. of 5.9040, which was almost the same as the statistical characteristic of the noise.

4. Discussion

A spike-sorting method based on automatic template reconstruction with a partial solution to the overlapping problem has been presented. After spike templates are reconstructed by using PCA and subtractive clustering techniques, a template-matching procedure is performed with the χ^2-test. The whole procedure is carried out without a priori knowledge, such as the standard spike waveforms or the firing time, i.e., it is a blind source separation method. Since template-matching is performed step by step together with the χ^2-test, once the template or templates combination that satisfies the three conditions shown in part 2.3.2 is found, it is unnecessary to check the remaining possible combinations of more templates. Thus, the computational effort is reduced, especially when there are many overlapping waveforms. At the same time, the over-fitting problem, especially when classifying overlapping waveforms, can be overcome to some extent. Simulation results demonstrated that the performance of our method is better than that of Atiya's (1992).

Noise is a complicating factor that hinders all spike sorting methods. We had not explored techniques for noise reduction. Because in our real experimental data the spectral characteristics of the noise and spikes were similar, it was
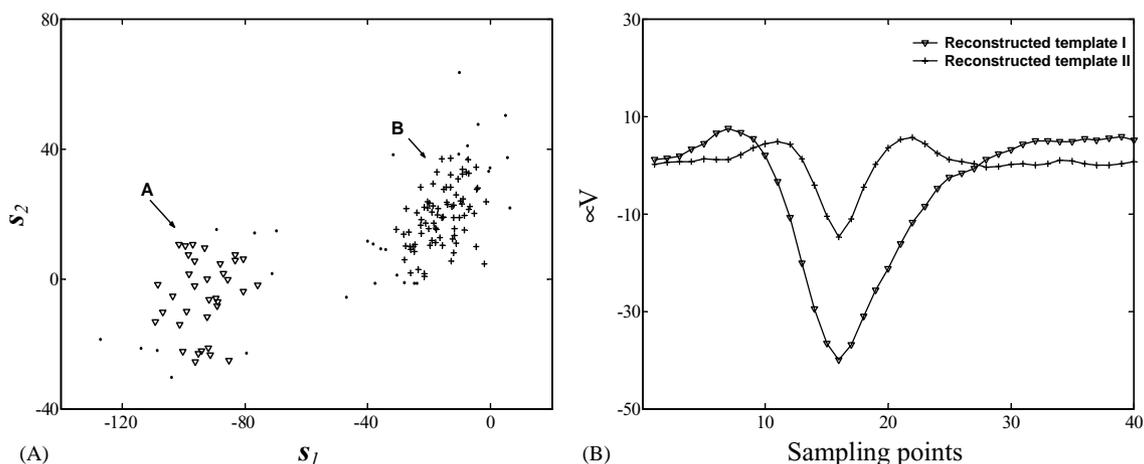

Fig. 9. (A) Scatter plot of scores s_1 and s_2 of the first two principal components. The first two principal components accounted for 74.1% of the data variation. After being analyzed by subtractive clustering method ($\gamma_a = 0.5$, $\gamma_b = 0.625$, the radius of each cluster was 20), two clusters were identified, i.e. (A) and (B). (B) Reconstructed templates I and II, which were the average waveforms of the spike events belonging to clusters (A) and (B) respectively.
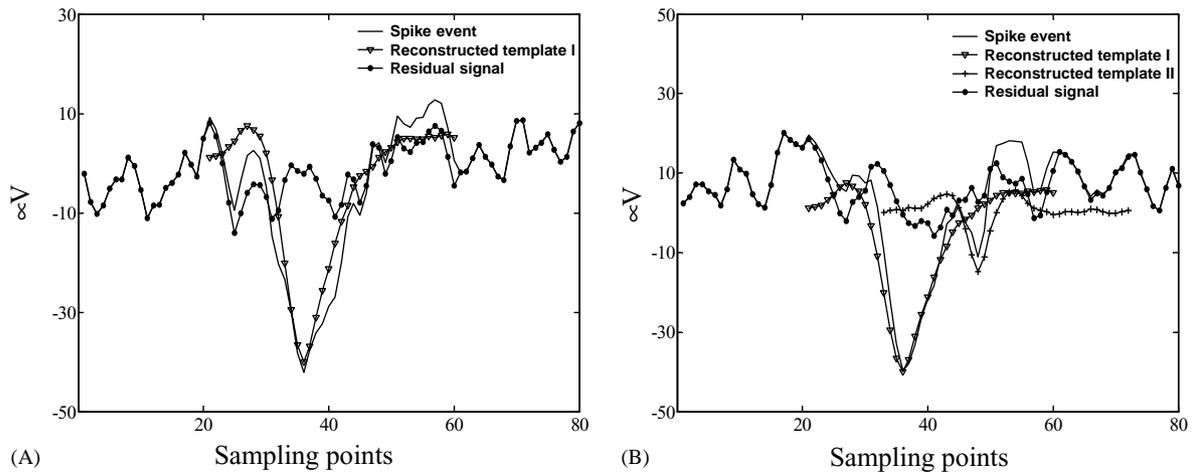
Fig. 10. Examples of spike sorting results. (A) This spike event was classified as reconstructed template I. The value of θ was 68.2802, which was within the range (64.1564, 96.4872), so the residue passed the χ^2-test and this event was well classified. (B) This spike event was classified as the combination of reconstructed templates I and II. The value of θ was 79.2729, which was within the range (64.1564, 96.4872), so the residue passed the χ^2-test and this event was well classified.

very difficult to apply noise reduction methods. In addition, it was not the central focus of this study. However, since the spike templates were reconstructed from the noise-smeared recording, noise level had some impact on the performance of this method. As shown in Fig. 4B, the reconstructed templates were still distorted by noise. The reliability of the reconstructed templates decreases as the signal-to-noise ratio decreases. We could have smoothened the waveforms of those reconstructed templates to reduce the noise affection, but the smoothness criterion is very difficult to determine.

The peak value was used as the feature to detect spike events, so that the selection of the threshold value had a strong impact on the performance of spike sorting method. If the threshold value is too large, spikes with small peak value will be missed. If the value is too small, the noise will be ex-

tracted as spurious spikes. Spikes in single-channel recordings may help to choose an appropriate threshold value.

The PCA technique was used to extract features from spike events. However, it should be emphasized that elements of Y were not normalized to have a mean of zero and an S.D. of one, which is required in the normal PCA. Because normalization will remove the general characteristics of each spike event, the differences in these events will be limited. Another reason is that all data were measured in the same unit (μV). Gwadry et al. (2001) also used this technique when analyzing brain image data. In our situation, when the spike events Y (the simulated data) were analyzed by the normal PCA, the first two principal components accounted for 72.9% of the data variation, while without normalization the first two principal components accounted for
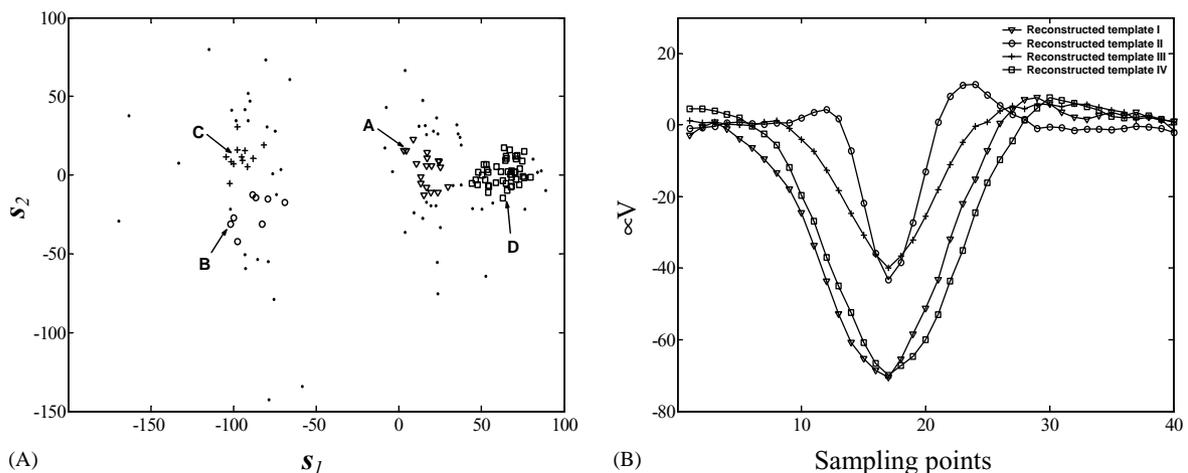

Fig. 11. Template reconstruction results when the spike events were analyzed by the normal PCA, which means that spike events were normalized to have a mean of zero and an S.D. of one. (A) Scatter plot of scores s_1 and s_2 of the first two principal components. The first two principal components accounted for 72.9% of the data variation. After being analyzed by subtractive clustering method ($\gamma_a = 0.2$, $\gamma_b = 0.25$, the radius of each cluster was 20), four clusters were identified, i.e. (A–D). (B) Reconstructed templates. Reconstructed templates were the average waveforms of the spike events belonging to corresponding clusters. The reconstructed templates were worse than those shown in Fig. 4B.

87.6%. The scatter plot of scores of the first two principal components obtained by using normal PCA together with the clustering result are shown in Fig. 11A. Template reconstruction results are shown in Fig. 11B, and it is clear that the reconstructed templates are worse than those shown in Fig. 4B.

The methods of *C*-means (also called *K*-means, Isodata), fuzzy *C*-means (also called fuzzy *K*-means, Fuzzy Isodata) have been the dominant approaches in both theoretical and practical application to unsupervised classification. For example, in spike sorting, Atiya (1992) used Isodata clustering algorithm, Zouridakis and Tam (2000) used fuzzy *K*-means clustering algorithm. However, these approaches are essentially iterative techniques that generate membership grades by using cluster centers and use the grades to induce new cluster centers. One difficulty with these approaches is the estimation of the initial values of the cluster centers. This fact, together with the local minimizing property of the algorithms, can sometimes complicate the process of clustering. Yager and Filev (1994) proposed the mountain clustering algorithm, which is based upon a gridding on the space, the construction of a mountain function from the data and then a destruction of the mountains to obtain the cluster centers. It is a simple and effective approach for approximate estimation of the cluster centers, but it has the drawback of being computationally expensive. Chiu and Cheng (1994) proposed the subtractive clustering method. The only difference is that in the subtractive clustering method the data are the candidates of cluster centers and not the gridding on the space. Therefore, the computational effort is reduced. The subtractive clustering method is quite robust if the clusters are roughly spherical and if suitable values of γ_a and γ_b can be found (Davé and Krishnapuram, 1997). Since in our experiments the noise followed Gaussian distribution, the clusters were spherical, and we therefore chose the subtractive clustering method. However, the values of γ_a and γ_b are critical for the correct implementation of the method. A large value for γ_a will merge clusters into big clusters, while a small value will split clusters into small spurious clusters. In our implementation of the algorithm, these values were chosen on the basis of a careful examination of the algorithm's performance on various data sets.

In this study, the template of each neuron was reconstructed as the average waveform of the spike events belonging to each cluster as other clustering analysis methods do (Lewicki, 1998). This procedure is still under improvement. The waveforms of spike events are distorted by noise in diverse extents. As shown in Fig. 4A, the point referring to the little distorted spike event is in the central area of the cluster, while the point referring to the overlapping waveform is far away from all of the clusters centers. The distance between each point and the cluster center may be used to define a weight when reconstructing the waveform of each cluster. But how to define the weight remains an open problem.

Acknowledgements

References

Atiya AF. Recognition of multiunit neural signals. IEEE Trans Biomed Eng 1992;39:723–9.

Chen AH, Zhou Y, Gong HQ, Liang PJ. Chicken retinal ganglion cells response characteristics: multi-channel electrode recording study. Sci China (Ser C) 2003;33:82–8.

Chiu S, Cheng JJ, Automatic rule generation of fuzzy rule base for robot arm posture selection. In: Proceedings of the NAFIPS Conference. San Antonio, TX, December; 1994. p. 436–40.

Davé RN, Krishnapuram R. Robust clustering methods: a unified view. IEEE Trans Fuzzy Sys 1997;5:270–93.

Gwadry, F., Berenstein, C, Horn JV. Implementation and application of principal component analysis on functional neuroimaging data. Technical Research Report. http://www.isr.umd.edu/TechReports/ISR/2001/TR_2001-47/TR_2001-47.phtml, 2001, pp. 1–27.

Letelier JC, Weber PP. Spike sorting based on discrete wavelet transform coefficients. J Neurosci Methods 2000;101:93–106.

Lewicki MS. Bayesian modeling and classification of neural signals. Neural Comput 1994;6:1005–30.

Lewicki MS. A review of methods for spike sorting: the detection and classification of neural action potentials. Network 1998;9:R53–78.

Pouzat C, Mazor O, Laurent G. Using noise signature to optimize spike-sorting and to assess neuronal classification quality. J Neurosci Methods 2002;122:43–57.

Salganicoff M, Sarna M, Sax L, Gerstain GL. Unsupervised waveform classification for multi-neural recordings: a real-time, software based system. I. Algorithms and implementation. J Neurosci Methods 1988;25:181–8.

Sarna MF, Gochin P, Kaltenbach J, Salganicoff M, Gertein GL. Unsupervised waveform classification for multi-neural recordings: a real-time, software based system. II. Performance comparison to other sorters. J Neurosci Methods 1988;25:189–96.

Yager RR, Filev DP. Approximate clustering via the mountain method. IEEE Trans Sys Man Cybernet 1994;24:1279–84.

Zouridakis G, Tam DC. Multi-unit spike discrimination using wavelet transforms. Comput Biol Med 1997;27:9–18.

Zouridakis G, Tam DC. Identification of reliable spike templates in multi-unit extracellular recordings using fuzzy clustering. Comput Methods Prog Biomed 2000;61:91–8.